SÍSMICA 2024
13º Congresso Nacional de Sismologia e Engenharia Sísmica

ANALYSING FRAGILITY CURVES DERIVED USING ALTERNATIVE GROUND MOTION SELECTION PROCEDURES

DESPOINA SKOULIDOU
Researcher
Resilience Guard GmbH

XAVIER ROMÃO
Assistant Professor
FEUP

SUMÁRIO

As curvas de fragilidade são um elemento essencial na avaliação do risco sísmico de estruturas e das correspondentes perdas. Neste contexto, o estudo desenvolvido explora as diferenças que podem ocorrer em curvas de fragilidade desenvolvidas a partir da resposta estrutural obtida utilizando dois métodos de análise diferentes: Análise para Múltiplas Intensidades (Multiple Stripe Analysis - MSA) e Análise Dinâmica Incremental (Incremental Dynamic Analysis - IDA), estando cada método associado a um procedimento diferente para seleção dos acelerogramas a utilizar. No caso do MSA, foram definidos diferentes grupos de acelerogramas compatíveis com diferentes Espectros Condicionais para as várias intensidades da análise. No caso da IDA, foi definido apenas um grupo de acelerogramas compatíveis com o espectro do EC8 associado à ação sísmica de projeto, os quais foram escalados de forma a cobrir os níveis de intensidade sísmica necessários. As diferenças encontradas nas curvas de fragilidade obtidas pelas duas abordagens refletem os diferentes pressupostos da seleção e escalamento dos acelerogramas utilizados para gerar os modelos de resposta estrutural, e permitem identificar condições em que os dois modelos de resposta conduzem a curvas de fragilidade comparáveis. Os resultados fornecem novos resultados acerca da importância do escalamento de acelerogramas e destacam a importância do uso de procedimentos adequados para a seleção dos acelerogramas.

ABSTRACT

Fragility curves are a fundamental component for developing risk and loss assessments of structures. This study explores potential differences found in analytical fragility curves obtained when considering two alternative analysis approaches: Multiple Stripe Analysis (MSA) and Incremental Dynamic Analysis (IDA), each associated with a different ground motion selection procedure. In case MSA is used, different groups of ground motions compatible with different Conditional Spectra are selected for the various stripes of the analysis, whereas in case IDA is used, a group of EC8 spectrum-compatible ground motions is selected for the design earthquake level and then scaled to cover the required range of seismic intensities. Differences found in the fragility curves derived by the two approaches reflect the different selection and scaling assumptions made for the ground motions used to obtain each demand model and allow identifying conditions where the two demand models lead to comparable fragility curves. The results provide new insights on the importance of ground motion scaling and highlight the importance of using adequate ground motions selection procedures.

KEYWORDS: Incremental dynamic analysis, multiple stripe analysis, performance levels, fragility curves, conditional spectrum, EC8 response spectrum

1. INTRODUCTION

Analytical fragility curves are a fundamental component for developing risk and loss assessments of structures, that can be especially useful when empirical and/or experimental data is scarce or non-existent. Developing analytical fragility curves requires analysing a structural model for multiple seismic intensity levels to derive the response-intensity relationship (also known as the Engineering Demand Parameter EDP – Intensity Measure IM relationship) and subsequently post-processing the results to define the evolution of the probability of reaching a certain performance level of interest for increasing levels of seismic intensity. There are currently three widely used analysis frameworks to establish the Probabilistic Demand Models (PDMs) and derive the EDP-IM relationship of structures using non-linear dynamic analysis: the Incremental Dynamic Analysis IDA [1], the Multiple Stripe Analysis MSA (e.g., [2]), and the cloud analysis [3]. All three approaches require the numerical simulation of the structure under investigation to represent its structural behaviour from linear elastic up to collapse, and the excitation of this simulation with one or more groups of Ground Motions (GMs) for various intensity levels. The main differences between the alternative approaches, which has been proven to affect the EDP-IM output, lie in the procedure for selecting group/s of GMs and for scaling them to cover the required intensity levels. Detailed descriptions of the three alternative approaches and relevant discussions can be found in existing literature (e.g., [4], [5]). In the following, findings related to IDA and MSA will be further discussed.

Luco and Bazzurro [6] showed that scaling a group of GMs with SFs as large as 10 or more could overestimate the structural response due to the non-representative GM frequency content and duration for intensities much different than the one that they have been recorded for, while similar remarks were made by Davalos and Miranda [7] for the collapse probabilities. Contradictory results were presented by Zacharenaki et al. [8] who showed that the structural response bias introduced by IDA using SFs up to 18.2 was small and acceptable for the buildings analysed in their study. Moving beyond EDPs, Pang and Wang [9] and Jin et al. [10] compared fragility curves constructed from IDA and MSA results and stated that the MSA results were more accurate, while the bias observed for the IDA curves was attributed to the excessive scaling of the GMs involved in IDA. It is worth mentioning that none of the previously mentioned studies accounted for spectral matching for a range of periods during the GM selection procedure, while only the spectral acceleration in the fundamental period of vibration ($Sa(T_1)$) was considered as an IM in some of them. On this respect, Korhangi et al. [11] compared fragility curves from IDA and MSA results and showed that the use of GMs without spectral and hazard consistency could lead to bias. In the referred study, the bias was towards overestimation for the IDA results. Yet it was highlighted that the overestimation could not be generalised.

Based on the above, the SF, the sufficiency of the IM, and the spectral shape control seem to be the key aspects for the discrepancies that appear between the fragility curves developed based on results from different approaches to establish the PDMs. To provide additional insights on the matter, the present study provides further results and discusses differences found at the fragility curve level when these are constructed considering two alternative PDMs based on IDA and MSA. By adopting the same fragility curve fitting technique for both PDMs, the referred differences will only reflect the selection and scaling assumptions made for the GMs used to obtain each demand model. Three RC buildings are simulated and analysed according to the two alternative approaches. The response results are subsequently post-processed and fragility curves are created for several limit states. The comparison of the results identifies the conditions where the two demand models lead to comparable fragility curves as well as possible limitations of each model.

2. CASE STUDY DESCRIPTION

2.1. Analysed buildings and numerical modelling

Three RC buildings with infilled frame structural systems, designed for gravity loads, are analysed herein. The buildings are located in Lisbon, Portugal and comprise 3-, 4- and 5-storey buildings, regular both in plan and in elevation. Fig. 1 shows the plan view of a typical storey of the buildings and the design details. The structural configuration, material characteristics, loading assumptions and the numerical simulation of the buildings have been previously presented in [12] and are omitted here due to length restrictions.

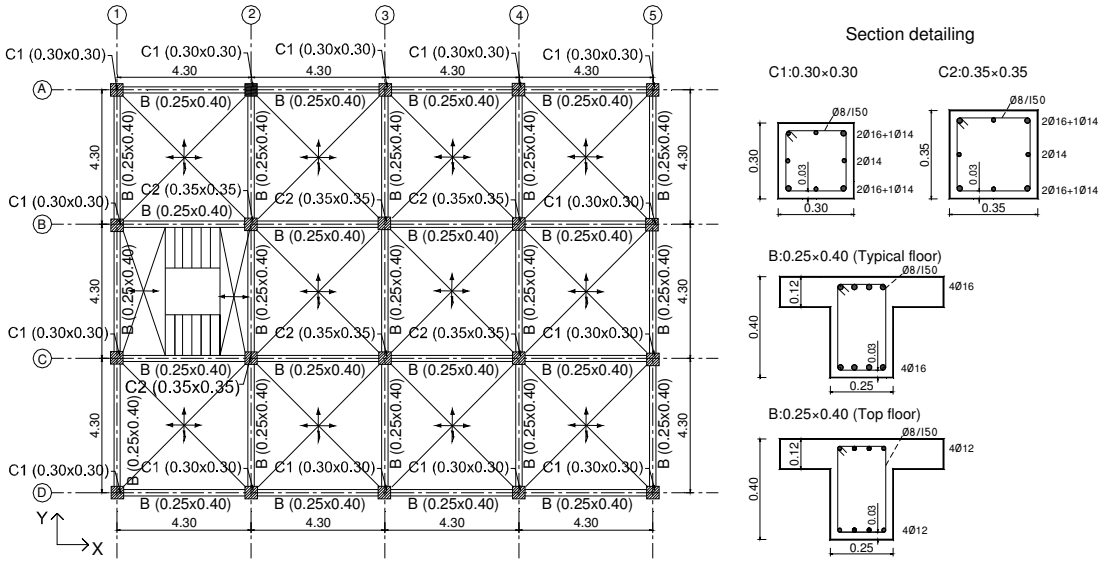

Fig. 1 - Plan view of a typical storey of the 3-storey, 4- storey and 5- storey buildings and the design details (all dimensions are in m).

The structural periods of the buildings along X and Y structural directions, with and without the masonry infills, as well as the average period T^* are presented in Table 1.

Table 1 - First and second mode periods of vibration of the buildings.

Period (s)\Building	3-storey	4-storey	5-storey
T_1,T_2 (infilled frame)	0.31,0.25	0.41,0.31	0.52,0.39
T_1,T_2 (bare frame)	0.73,0.72	0.96,0.93	1.18,1.15
T^*	0.50	0.66	0.82

2.2. Ground motion selection

The ground motion selection procedures are presented in this section for the two PDMs. In both cases the geometric mean was used as the representative component for each bi-directional GM. For the MSA, the probabilistic seismic hazard analysis of the site (Lisbon) was initially performed using the SelEQ software [13] and the annual seismic hazard curve was subsequently determined for the period T^* of each building. Disaggregation of the hazard was then performed for four probabilities of exceedance, i.e., 50%, 10%, 5% and 2% in 50 years, at T^* and the results were used to build four conditional spectra (CS). After a preliminary ground motion record selection based on seismological and strong motion parameters, the final selection of a group of 40 bi-directional records was performed by ensuring compatibility between the target spectrum, i.e., the CS, and the group of records. Compatibility was achieved by

minimizing the difference between statistics (i.e., the mean and standard deviation of the logarithms of the spectral accelerations) of the target spectrum and the same statistics of the group in a period range of 0.2T^*-1.5T^* (see [13] for more details). An additional criterion was included in the process which involves minimizing also the skewness of the logarithms of the spectral accelerations to a value close to zero for the same period range. Furthermore, the SFs used for each individual GM were restricted to the 0.25-4.00 range. Ultimately, four groups of 40 GMs, each corresponding to a different probability of exceedance (i.e., a different CS), were selected for each building.

For the IDA, one group of 40 bidirectional GM records was selected according to the EC8 provisions using the Type 2 elastic response spectrum with a 5% viscous damping. The parameters of the EC8 response spectrum used for the GM selection procedure are provided in Table 2, where a_g is the design ground acceleration for soil type A and zone 2.3 in Portugal, S is the soil factor for soil type B, and T_b, T_c and T_d are the corner periods. Criteria related to seismological and strong motion parameters, such as M, R and V_{S30} were taken into account when performing the preliminary GM selection. Subsequently, the GM selection was performed by ensuring compatibility between the group mean and individual response spectra and the target response spectrum in a period range of 0.2 T^*-1.5T^*. The spectral mismatch between the mean of the group and the target response spectrum was limited to the interval of ±10%, while the spectral mismatch between the individual spectrum of each record and the target spectrum was limited to ±50%. The SFs used for each individual GM were restricted to the 0.25-4.00 range.

Table 2 - EC8 Type 2 response spectrum parameters.

RS	a_g (m/s^2)	S	T_b (s)	T_c (s)	T_d (s)
Type 2	1.7	1.27	0.1	0.25	2

The mean spectrum (and dispersion) of the 40 GMs matched to the CS for each probability of exceedance and the mean spectrum (and dispersion) of the 40 GMs matched to the EC8 spectrum are shown in Fig. 2, Fig. 3 and Fig. 4 for the 3-storey, the 4-storey and the 5-storey buildings, respectively. The target CS and the EC8 spectrum are also presented in the same figures for comparison. Note that the GMs selected to match the EC8 spectrum are the same for all buildings and for all intensities. The mean spectrum of the EC8-compatible GM group, which is originally matched to the EC8 spectrum with 10% probability of exceedance in 50 years, is multiplied by appropriate SFs to reach the intensity of the other three probabilities of exceedance at Sa(T^*) for each building. In the comparison of response spectra presented in the following, focus should be given to period ranges that are expected to govern the behaviour of the structures for different damage states. Therefore, for low damages states, spectral comparisons should focus on the period range below, but close to, T^* which involve spectral values with higher probabilities of exceedance. On the contrary, for high damages states, spectral comparisons should focus on the period range above, but close to, T^* which involve spectral values with lower probabilities of exceedance.

Starting from the comparison of the target spectra, the target CS and the EC8 spectrum are seen to present some differences that vary with the probability of exceedance and with the building (i.e., T^*). Generally, the differences appear to be more pronounced for the higher probabilities of exceedance, while they reduce for the lower probabilities of exceedance for all buildings. Focusing on the lower period range (i.e., below, but close to, T^*), the CS is always associated with higher spectral accelerations for the 30% and 10% probability of exceedance in 50 years, whereas this effect reduces for the lower probabilities of exceedance. For the 2% probability of exceedance in 50 years the two spectra coincide in this period range for all three buildings. The opposite trend is observed for the higher period range (i.e., above, but close to, T^*). While for higher probabilities of exceedance the CS is associated with smaller spectral accelerations when compared to the EC8 spectrum, for the lower probabilities of exceedance this mismatch decreases and, in some cases, the trend is inverted. An illustrative example

of this last observation can be seen in Fig. 2d with the spectra for the 3-storey building, in which the red continuous line, i.e., the CS, is above the black continuous line, i.e., the scaled EC8 spectrum, for the referred period range.

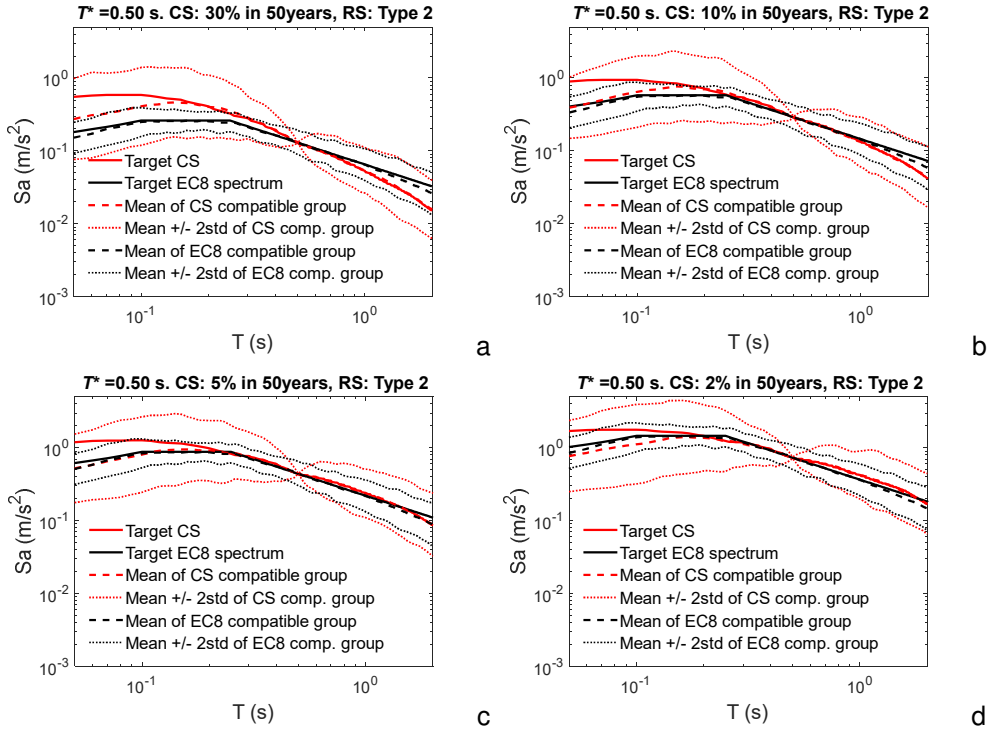

Fig. 2 - Comparison of response spectra of the group of GMs selected for the 3-storey building according to the CS (a. 30% in 50 years, b. 10% in 50 years, c. 5% in 50 years and d. 2% in 50 years) and the EC8 spectrum. The target CS and EC8 spectrum are plotted for reference.

With respect to the comparison of the mean of each group with the respective target spectra, very good matching trends are observed for the period range of interest. The EC8-compatible group follows very closely the target EC8 spectrum for the whole period range, while some deviations start appearing for periods larger than1.5s that are beyond the period range of interest for all buildings. The CS compatible groups, on the other hand, match very well the target CS for all periods above ~0.1-0.2s. Since the lowest period of interest is 0.1s, i.e., 0.2T^* for the 3-storey building, matching is also considered adequate. As a result, it can be seen that the average spectra follow trends similar to those of the target spectra, demonstrating the validity of the selection process and indicating that the differences between the mean spectra of the groups stem mostly from the different target spectra they were matched to. In contrast to the mean spectrum, the dispersion of the groups presents significant differences. With the exception of the narrow range very close to T^* where the CS-compatible group has very low dispersion, as expected since all GMs have been selected and scaled to pass through Sa(T^*), the EC8-compatible group has either comparable or much lower dispersion for all other periods, when compared to that of the CS-compatible groups. Extreme cases are observed for the 30% probability of exceedance of all buildings (see Fig. 2a, Fig. 3a, Fig. 4a), where both the mean spectrum and the dispersion have much higher Sa values for periods smaller than T^*. Unlike the previous observations, very good matching is observed, both for the mean spectra and the dispersion, for the 2% probability of exceedance CS-compatible group and the EC8-compatible group of the 5-storey building (see Fig. 4d). It is noted that the different dispersion between the GM groups selected according to the different approaches is due to the different assumptions considered during the GM selection process.

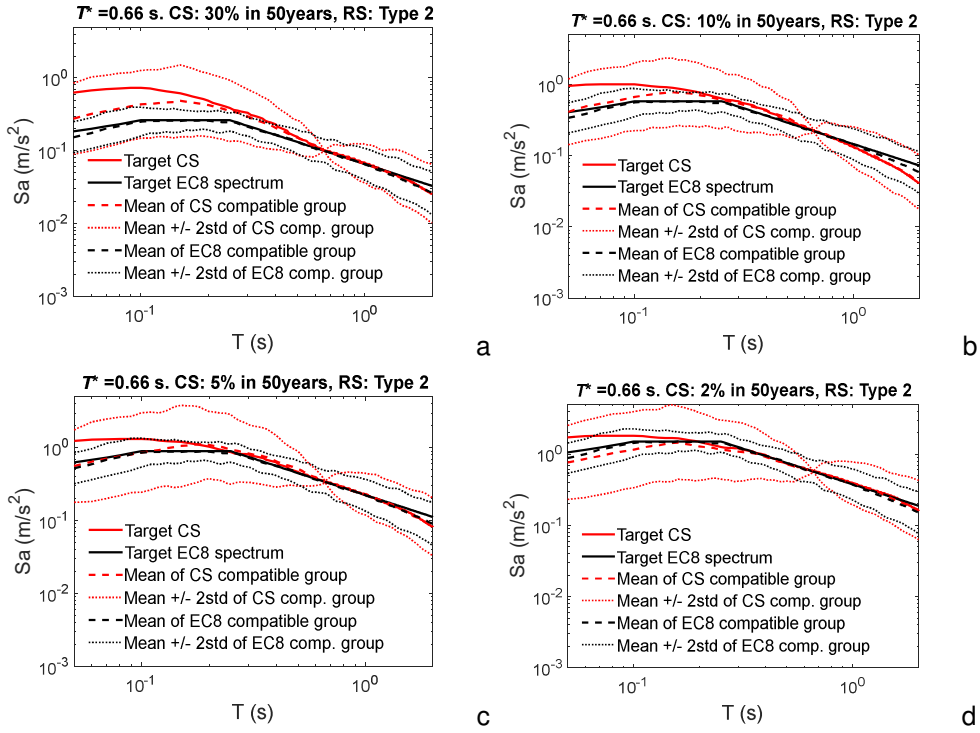

Fig. 3 - Comparison of response spectra of the group of GMs selected for the 4-storey building according to the CS (a. 30% in 50 years, b. 10% in 50 years, c. 5% in 50 years and d. 2% in 50 years) and the EC8 spectrum. The target CS and EC8 spectrum are plotted for reference.

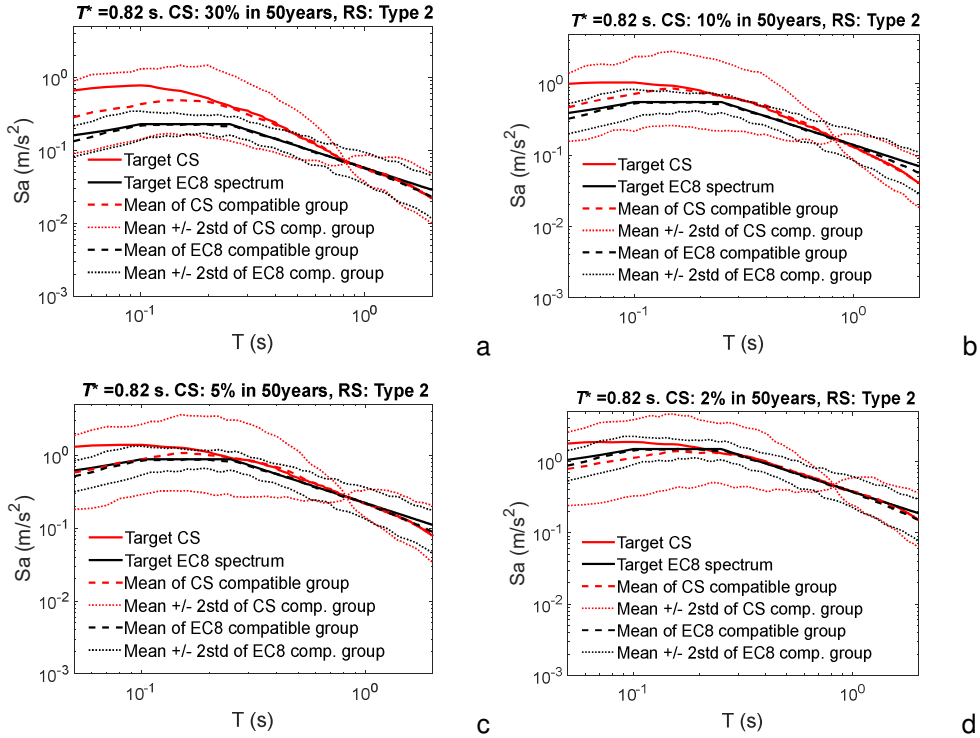

Fig. 4 - Comparison of response spectra of the group of GMs selected for the 5-storey building according to the CS (a. 30% in 50 years, b. 10% in 50 years, c. 5% in 50 years and d. 2% in 50 years) and the EC8 spectrum. The target CS and EC8 spectrum are plotted for reference.

3. PROBABILISTIC DEMAND MODELS

The two alternative PDMs obtained from the structural analyses are presented in this section, highlighting the implemented SFs. Both IDA and MSA analyses are performed using Sa(*T**) as the control IM. Structural collapse is associated to the occurrence of a very large interstorey drift (ISD) ratio (>10%) or numerical failure (non-convergence) of the model. For the MSA, the four GM groups selected for each building are scaled up and down to span a total of 20 intensity levels. The GM group selected for the 50% probability of exceedance in 50 years was applied along 4 intensities (using group SFs in the range of 0.38-1.54), the 10% in 50 years group was applied along 3 intensities (using group SFs in the range of 0.82-1.23), the 5% in 50 years group was applied along 4 intensities (using group SFs in the range of 0.89-1.39) and the 2% in 50 years group was applied along 9 intensities (using group SFs in the range of 0.91-1.97), eventually covering events with return periods of ~50 to 10000 years. Detailed information on the SFs and the return periods can be found in [14]. The overall SFs used for the GMs, which resulted from the combination of the group SFs and the individual SFs presented in Section 2.2 range from 0.11 to 7.84. IDA was performed by scaling the EC8-compatible group to capture structural response from elastic up to collapse. The SFs of the group ranged from 0.14 to 9.95. The overall SFs of the GMs (i.e., combination of the group SFs and the individual SFs presented in Section 2.2) range from 0.11 to 21.58, which is almost three times wider than the SF range used in MSA. Indicative analysis results (EDP-IM) obtained for the 3-storey building are presented in Fig. 5 and in Fig. 6 for the MSA (stripes of EDPs) and the IDA (IDA curves) PDM, respectively.

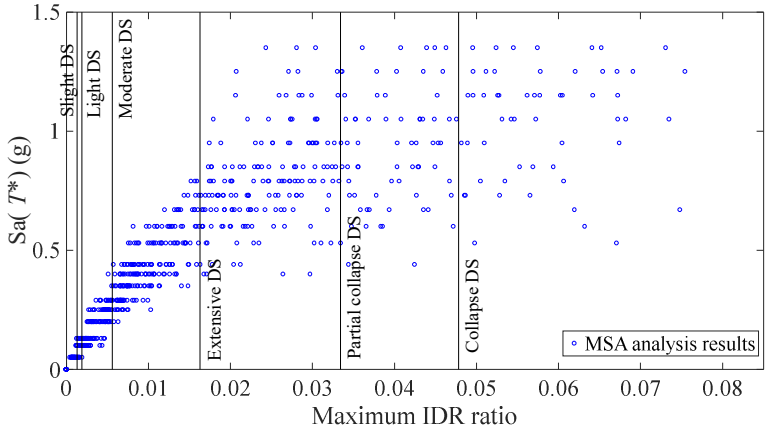

Fig. 5 - MSA analysis results (stripes) at the considered IM levels. Results for the 3-storey building. The vertical black lines represent the EDP thresholds for the considered DS.

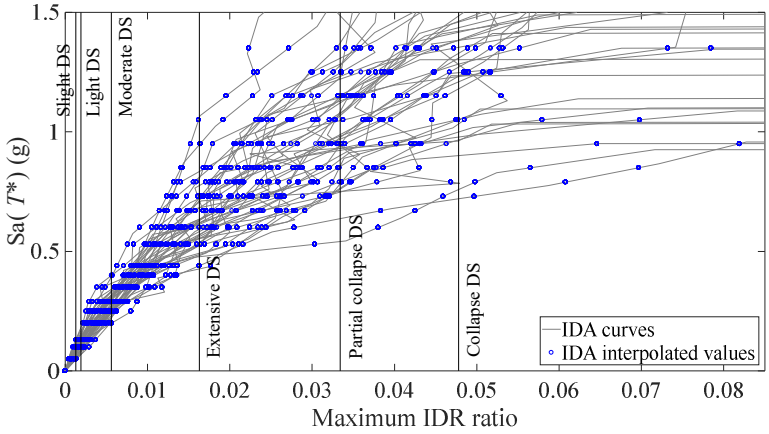

Fig. 6 - IDA curves and interpolated values at the considered IM levels. Results for the 3-storey building. The vertical black lines represent the EDP thresholds for the considered DS.

4. FRAGILITY CURVE DEVELOPMENT AND COMPARISON

4.1. Development of fragility curves

The EDP-based approach is used to fit fragility curves to the structural analysis results. According to this approach, the number of analyses that cause failure with respect to a predefined threshold at each IM level are initially identified and the binomial distribution is used to evaluate the likelihood of having the observed number of failures, k_i, out of the total number of analyses, n_i, at a given IM level i:

$$\mathrm{P}(k_i failures\ in\ n_i analyses) = \binom{n_i}{k_i} {p_i}^{k_i}(1-p_i)^{n_i-k_i} \quad (1)$$

where, p_i is the probability that an analysis at a given IM will lead to failure. When such data is available at multiple IM levels, a likelihood function can be obtained as the product of the binomial probabilities at each IM level. The p_i, values are assumed to be defined by the cumulative distribution function of a lognormal distribution whose parameters, i.e., θ and β, where θ is the median and β is the standard deviation of the log of the data, are evaluated using the maximum likelihood estimation method. Furthermore, the maximum ISD ratio is used as the EDP and the thresholds of six Damage States (DS) are defined according to Rossetto and Elnashai [15], shown in Table 3. It is noted that adopting DS thresholds defined for structures other than the ones analysed can be inaccurate and potentially dangerous, especially if the referred DSs are associated with expected losses. Nevertheless, since the purpose of the present study is to compare fragility curves derived from alternative approaches, the latter is not seen as a concern and the Rossetto and Elnashai [15] DSs can be used for the comparative analysis.

Table 3 - Damage states definition and threshold values of maximum ISD ratios [15].

Damage state	Slight DS1	Light DS2	Moderate DS3	Extensive DS4	Partial Collapse DS5	Collapse DS6
Max ISD ratio %	0.13	0.19	0.56	1.63	3.34	4.78

The adopted EDP-based fragility estimation requires that EDPs are obtained in distinct IM levels, i.e., in stripes. This requirement is satisfied by default in the MSA demand model (see Fig. 5 for the 3-storey building), as GMs are selected for specific IM levels with predefined probabilities of exceedance, while in IDA some post processing of the analysis results needs to be performed. As such, the IDA curves are constructed for all GMs involved in the IDA demand model and are used to obtain EDP stripes at specific IM levels by interpolation. For consistency, interpolation was performed at the IM levels used for the MSA. Fig. 6 shows the IDA curves developed for the 3-storey building and the interpolated EDP values at the IM levels considered for the MSA of the same building. The vertical lines in Figure 7 represent the DS thresholds presented in Table 3.

Fragility curves are created for the three buildings according to the previously presented EDP-based approach for both MSA and IDA using a lognormal distribution for the six DSs. Fig. 7, Fig. 8, and Fig. 9 show the fragility curves developed for the 3-storey, 4-storey, and 5-storey building, respectively. As a side note, it has been stated in [16] that for the estimation of the parameters of the lognormal distribution using the aforementioned approach, i.e., the maximum likelihood method, all GMs at the multiple IM levels should be independent. Nevertheless, according to the same research, the violation of this requirement has small effects on the estimated parameters and can be thus used even with IDA results, as in the present study.

4.2. Fragility curves comparison

It can be seen that for the three lower DSs, Slight, Light and Moderate, there are insignificant differences between the fragility curves created using the IDA and the MSA PDM and this observation is valid for all three buildings analysed. Still, the MSA fragility curves exhibit an almost imperceptible shift towards conservatism. At the same time the fragility curves for these three DSs are quite vertical, i.e., they exhibit low dispersion. The reason for this low dispersion is attributed to the small number of stripes that contribute to the fragility curves of these DSs and their close values (the rest of the stripes lead to either 0 or 100% probability of exceedance). This effect is demonstrated in Fig. 5 and Fig. 6 which show the threshold EDP values for all DSs (vertical black lines) on top of the EDP stripes. The DS1 and DS2 EDP thresholds intersect only three stripes, while the DS3 EDP intersects four stripes, still with close Sa(*T**) values.

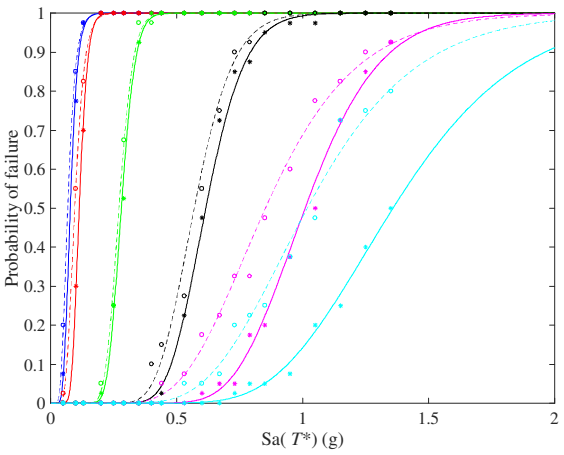

DS	MSA/IDA parameters θ	β
DS1	0.07/0.08	0.35/0.29
DS2	0.10/0.11	0.31/0.22
DS3	0.27/0.28	0.16/0.16
DS4	0.57/0.62	0.21/0.20
DS5	0.85/1.01	0.33/0.23
DS6	1.02/1.36	0.33/0.29

Fig. 7 - Fitted fragility curves and parameters of the lognormal model for the two alternative probabilistic demand models and the six DSs for the 3-storey building.

Despite the similarity of the fragility curves of these DSs (Slight, Light and Moderate) for the two alterative PDMs, the fractions of analysis causing failure for the individual IM values present differences. These differences can be seen in Fig. 7, Fig. 8 and Fig. 9, which show the fractions of analyses that led to failure on top of the fitted curves. It can be observed that for DS1, DS2 and DS3 and for each individual IM that has not led to a 0 or 100% probability of failure, the MSA approach led to higher fractions compared to IDA. For instance, in Fig. 9 and for the first IM which is equal to 0.05g, the fraction of analyses that led to failure according to MSA is 0.2, while for IDA it is less than 0.1. Similar observations can be made for the next two IMs as well. It is also worth noting that these differences, i.e., the higher fractions of the MSA compared to IDA, can be associated with the GM spectral shapes presented in Section 2.2. The analysis of the four lowest stripes, that contribute to the development of the fragility curves of DS1 and DS2, was performed using the GM group compatible with the 30% in 50 years CS for the MSA. The comparison of this spectrum with that of the EC8-compatible group that was used to perform the IDA, shown in Fig. 2a, Fig. 3a and Fig. 4a for the three buildings, reveals that, for spectral accelerations close to the period of vibration of the infilled structures (i.e., the period that the structures are expected to exhibit for these low IMs), the mean spectrum of the CS-compatible group is above the mean spectrum of the EC8-compatible group, while the dispersion of the former is much larger and mainly towards overestimation.

The discrepancies between the fragility curves created using the alternative PDMs are mainly observed for the three highest DSs, i.e., Extensive, Partial Collapse and Collapse, with differences increasing with the severity of the DS and with different trends among the different buildings. The smallest differences are observed for the 5-storey building,

presented in Fig. 9. No remarkable differences can be seen for the fragility curves of the Extensive DS, while the MSA PDM results in a slightly more conservative fragility curve for the Partial Collapse DS and in slightly higher dispersion for the Collapse DS. Nevertheless, the observed differences can be characterised as minimal. These trends can be associated with the spectral shapes presented in Fig. 4c and 4d, since the intensities that contribute to the fragility curves for these three DS are the ones associated with the 5% and 2% in 50 years CS for the MSA. For periods close to T^* and slightly larger than T^*, the two mean spectra are similar. Furthermore, the similar variation of the two groups around the mean spectra provides evidence for the similarity of the fragility curves. It is also noted that despite the much larger, almost three times, SFs used for the highest DS in IDA, no relevant overestimation is observed.

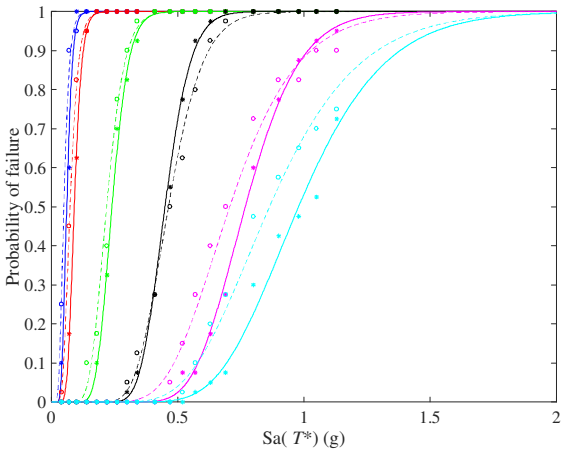

DS	MSA/IDA parameters θ	β
DS1	0.05/0.06	0.35/0.28
DS2	0.07/0.09	0.34/0.26
DS3	0.22/0.24	0.25/0.22
DS4	0.46/0.45	0.23/0.18
DS5	0.71/0.76	0.29/0.22
DS6	0.86/0.98	0.31/0.27

Fig. 8 - Fitted fragility curves and parameters of the lognormal model for the two alternative probabilistic demand models and the six DSs for the 4-storey building.

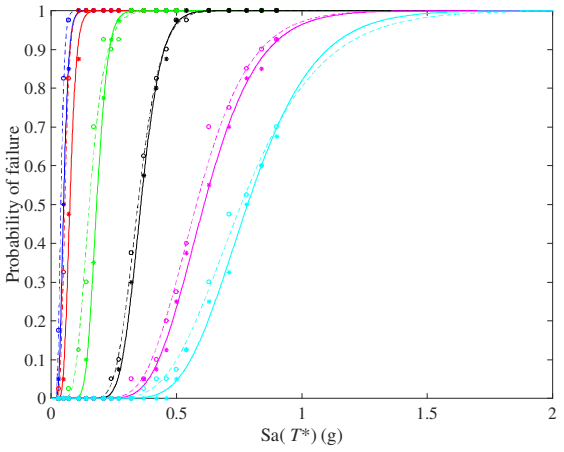

DS	MSA/IDA parameters θ	β
DS1	0.04/0.05	0.28/0.30
DS2	0.05/0.07	0.27/0.28
DS3	0.15/0.18	0.31/0.19
DS4	0.35/0.36	0.21/0.18
DS5	0.58/0.61	0.29/0.27
DS6	0.76/0.78	0.32/0.27

Fig. 9 - Fitted fragility curves and parameters of the lognormal model for the two alternative probabilistic demand models and the six DSs for the 5-storey building.

The Extensive DS fragility curves of the 3- and 4-storey buildings present small differences, the former in the median and the latter in the variability, while the Partial Collapse and the Collapse DS fragility curves are the ones mostly affected by the different PDMs. For both buildings, fragility curves derived using the MSA PDM are associated with lower IM levels, and are hence more conservative, while a slight difference in the slope is also observed for the Partial Collapse DS, with the MSA leading to higher dispersion (curves with lower slope). Based on the same rationale, the

differences between the fragility curves of the 3-storey and the 4-storey buildings can be associated with the response spectra (mean and dispersion) of the 5% and 2% in 50 years probability of exceedance. In both cases, the average spectrum of the CS-compatible group presents slightly higher Sa values with respect to the average spectrum of the EC8-compatible group and for periods larger than, but close to, *T**. As it has already been explained, the buildings are expected to respond with periods closer to the bare frame, and thus larger than *T** for the higher intensities, as those associated with the DS of partial collapse and collapse. The variability of the group spectra is also higher for the CS compatible ones and always towards higher Sa values, hence further supporting the conservatism of the MSA PDM. The higher variability of the spectra of the CS-compatible groups can be reflected in the higher β parameters of the lognormal model (i.e., the standard deviation of the logarithmic values) of the MSA fragility curves compared to their IDA counterparts. Last but not least, the much higher SFs used in IDA for the highest intensity levels do not seem to lead to overestimation of the corresponding fragility curves.

5. FINAL REMARKS

The study analysed differences between the fragility curves developed for three RC buildings using two alternative PDMs established using two different analysis approaches, the MSA and the IDA. By employing the same fitting technique for the development of the fragility curves in both PDMs, the referred differences were attributed to the GM selection and scaling procedures, which differed between the two PDMs.

The results showed a strong correlation between the mean spectra of the GM groups used for the two PDMs and the resulting fragility curves. The higher mean spectrum, i.e., higher Sa values, used for the MSA in comparison to the mean spectrum used for the IDA, appeared to lead to more conservative fragility curves in the former case. Simultaneously, the higher variability of the CS-compatible GMs was also reflected in the higher values of the β parameter of the MSA fragility curves when compared to those obtained for the IDA fragility curves. Furthermore, the much higher SFs used on the GMs for IDA did not seem to have an observable effect on the fragility curves compared to the lower SFs used on the GMs for the MSA, unlike discussed in previous studies. The effect of using different PDMs was found to vary among the several DSs and appeared to have minimal effects for the less severe DSs that were associated with very vertical fragility curves. Although the spectral shapes might suggest otherwise, the small range of IMs that contributed to the fragility curves managed to reduce the impact of these differences. Still, the fraction of analyses used to create the fragility curves revealed the higher conservatism of the MSA compared to the IDA results, as suggested by the average spectral shapes and their dispersion.

Overall, evidence was presented that both the mean spectral shape and the dispersion of the selected GM groups have an effect in the fragility curves and these were found to be the main sources of differences observed between the fragility curves developed for the alternative PDMs. The adoption of large SFs, on the other hand, did not seem to cause visible effects, as long as the spectral shape (average and dispersion) in the period range of interest was controlled. Although this was a preliminary attempt to identify and quantify the effects of using alternative PDMs, the results seem reasonable and in accordance with suggestions of relevant studies. Future research on this topic should investigate, in addition to the analysis of more buildings with different structural material and configurations (structural systems, with vertical and/or in-plan irregularities), fragility curves developed for the MSA and IDA using alternative fitting techniques (e.g., IM-based for IDA) and other analysis approaches (e.g., cloud analysis). Finally, the effect of using alternative PDMs could also be studied in terms of the resulting failure rates, i.e., the convolution of the fragility curves with the seismic hazard curve.

6. AKNOWLEDGEMENTS/FUNDING

This work is financially supported by national funds through the FCT/MCTES (PIDDAC), under the project DRI/India/0645/2020 – Evaluation and Retrofitting of Existing Buildings for Safe and Sustainable Built Environment https://doi.org/10.54499/DRI/India/0645/2020, and by Base Funding -UIDB/04708/2020 and Programmatic Funding- UIDP/04708/2020 of the CONSTRUCT -Instituto de I&D em Estruturas e Construções- funded by national funds through the FCT/MCTES (PIDDAC). The authors would like to thank the anonymous reviewer for their insightful comments.

7. REFERENCES

[1] Vamvatsikos, D., & Cornell, C.A. (2002). Incremental dynamic analysis. Earthq Eng Struct Dyn, 31(3), 491-514.
[2] Jalayer, F., & Cornell, C.A. (2009). Alternative non-linear demand estimation methods for probability-based seismic assessments. Earthq Eng Struct Dyn, 38(8), 951-972.
[3] Jalayer, F., De Risi, R., & Manfredi, G. (2015). Bayesian Cloud Analysis: efficient structural fragility assessment using linear regression. Bull Earthq Eng, 13, 1183-1203.
[4] Mackie, K.R., & Stojadinovic, B. (2005). Comparison of incremental dynamic, cloud, and stripe methods for computing probabilistic seismic demand models. In Structures Congress 2005: Metropolis and Beyond (pp. 1-11).
[5] Baltzopoulos, G., Baraschino, R., Iervolino, I., & Vamvatsikos, D. (2018). Dynamic analysis of single-degree-of-freedom systems (DYANAS): A graphical user interface for OpenSees. Eng Struct, 177, 395-408.
[6] Luco, N., & Bazzurro, P. (2007). Does amplitude scaling of ground motion records result in biased nonlinear structural drift responses? Earthq Eng Struct Dyn, 36(13), 1813-1835.
[7] Dávalos, H., & Miranda, E. (2019). Evaluation of the scaling factor bias influence on the probability of collapse using Sa (T1) as the intensity measure. Earthq Spectra, 35(2), 679-702.
[8] Zacharenaki, A., Fragiadakis, M., Assimaki, D., & Papadrakakis, M. (2014). Bias assessment in incremental dynamic analysis due to record scaling. Soil Dyn Earthq Eng, 67, 158-168.
[9] Pang, Y., & Wang, X. (2021). Cloud-IDA-MSA conversion of fragility curves for efficient and high-fidelity resilience assessment. J Struct Eng, 147(5), 04021049.
[10] Jin, A., Qiu, Y., & Wang, J. (2023). Comparison of seismic fragility analysis methods for arch dams. Earthq Eng Eng Vibr, 22(1), 173-189.
[11] Kohrangi, M., Vamvatsikos, D., & Bazzurro, P. (2017). Site dependence and record selection schemes for building fragility and regional loss assessment. Earthq Eng Struct Dyn, 46(10), 1625-1643.
[12] Skoulidou, D., & Romão, X. (2019). Uncertainty quantification of fragility and risk estimates due to seismic input variability and capacity model uncertainty. Eng Struct, 195, 425-437.
[13] Macedo, L., & Castro, J.M. (2017). SelEQ: An advanced ground motion record selection and scaling framework. Adv Eng Softw, 114, 32-47.
[14] Skoulidou, D., Romão, X., & Franchin, P. (2019). How is collapse risk of RC buildings affected by the angle of seismic incidence? Earthq Eng Struct Dyn; 48(14):1575-1594.
[15] Rossetto, T., & Elnashai, A. (2003). Derivation of vulnerability functions for European-type RC structures based on observational data. Eng Struct, 25(10), 1241-126.
[16] Baker, J. W. (2015). Efficient analytical fragility function fitting using dynamic structural analysis. Earthq Spectra, 31(1), 579-599.